ISSN 1674-1056
http://cpb.iphy.ac.cn
http://iopscience.iop.org/cpb
中国物理 B
Chinese Physics
中国物理 Chinese Physics B

Electrical controllable spin valves in a zigzag silicene nanoribbon ferromagnetic junction

Lin Zhang(张林)
Citation: Chin. Phys. B . 2018, 27(6): 067203. **doi:** 10.1088/1674-1056/27/6/067203

Journal homepage: http://cpb.iphy.ac.cn; http://iopscience.iop.org/cpb

What follows is a list of articles you may be interested in

Influence of spin-orbit coupling on spin-polarized electronic transport in magnetic semiconductor nanowires with nanosized sharp domain walls

Lian Liu(刘恋), Wen-Xiang Chen(陈文祥), Rui-Qiang Wang(王瑞强), Liang-Bin Hu(胡梁宾)
Chin. Phys. B . 2018, 27(4): 047201. **doi:** 10.1088/1674-1056/27/4/047201

Spin transport in a chain of polygonal quantum rings with Dresselhaus spin-orbit coupling

Han-Zhao Tang(唐翰昭), Xiao-Teng Yao(要晓腾), Jian-Jun Liu(刘建军)
Chin. Phys. B . 2017, 26(11): 117203. **doi:** 10.1088/1674-1056/26/11/117203

Coherent charge transport in ferromagnet/semiconductor nanowire/ferromagnet double barrier junctions with the interplay of Rashba spin–orbit coupling, induced superconducting pair potential, and external magnetic field

Li-Jie Huang(黄立捷), Lian Liu(刘恋), Rui-Qiang Wang(王瑞强), Liang-Bin Hu(胡梁宾)
Chin. Phys. B . 2017, 26(7): 077201. **doi:** 10.1088/1674-1056/26/7/077201

Current induced nonequilibrium spin polarization in semiconductor-nanowire/s-wave superconductor junctions with strong spin-orbit coupling

Nai-Qing Liu(刘乃清), Li-Jie Huang(黄立捷), Rui-Qiang Wang(王瑞强), Liang-Bin Hu(胡梁宾)
Chin. Phys. B . 2016, 25(2): 027201. **doi:** 10.1088/1674-1056/25/2/027201

Characteristics of anomalous Hall effect in spin-polarized two-dimensional electron gases in the presence of both intrinsic, extrinsic, and external electric-field induced spin–orbit couplings

Liu Song,Yan Yu-Zhen,Hu Liang-Bin
Chin. Phys. B . 2012, 21(2): 027201. **doi:** 10.1088/1674-1056/21/2/027201

Electrical controllable spin valves in a zigzag silicene nanoribbon ferromagnetic junction*

Lin Zhang(张林)[1,2,†]

[1] Department of Applied Physics, College of Science, Nanjing Forestry University, Nanjing 210037, China
[2] Department of Physics and Institute of Theoretical Physics, Nanjing Normal University, Nanjing 210023, China

(Received 25 February 2018; revised manuscript received 25 March 2018; published online 10 May 2018)

We propose two possible spin valves based on a zigzag silicene nanoribbon (ZSR) ferromagnetic junction. By using the Landauer–Bütikker formula, we calculate the spin-resolved conductance spectrum of the system and find that the spin transport is crucially dependent on the band structure of the ZSR tuned by a perpendicular electric field. When the ZSR is in the topological insulator phase under a zero electric field, the low-energy spin transport and its ON and OFF states in the tunneling junction mainly rely on the valley valve effect and the edge state of the energy band, which can be electrically modulated by the Fermi level, the spin–orbit coupling, and the local magnetization. When a nonzero perpendicular electric field is applied, the ZSR is a band insulator with a finite energy gap, the spin switch phenomenon is still preserved in the device and it does not come from the valley valve effect, but from the energy gap opened by the perpendicular electric field. The proposed device might be designed as electrical tunable spin valves to manipulate the spin degree of freedom of electrons in silicene.

Keywords: zigzag silicene nanoribbon, spin valve, spin–orbit coupling, conductance

PACS: 72.25.Dc, 72.80.Vp, 72.25.Mk, 73.43.Qt **DOI:** 10.1088/1674-1056/27/6/067203

1. Introduction

Spintronics,[1,2] aiming to manipulate the charge and spin degrees of freedom of electrons in nanodevices, has received considerable interest from researchers due to its faster processing speed and lower energy consumption compared with traditional electronic devices.[3,4] Among the various materials of spintronics, graphene is more attractive owing to its unique two dimensional hexagonal lattice structure,[5] long spin relaxation time,[6] high carrier mobility,[7] and gate voltage controllable electron transport at room temperature.[8] In order to realize future graphene spin devices, various kinds of current valves controlled by electrical methods are becoming increasingly important for their convenience in practice and the advantage that the electric field cannot break the spin coherence in devices.[9,10] Because the bulk graphene is a gapless semiconductor, it is difficult to electrically modulate the carrier transport around the Dirac point for the Klein paradox,[10] until the valley valve effect or band selective transport was found in the zigzag graphene nanoribbon (ZGR) junction.[11]

The valley valve effect offers an efficient electrical way to manipulate the inter-valley electron transport in graphene by using so-called pseudo-parity conservation.[11–17] For example, Rycerz *et al.*[11] first proposed a gate tunable current valve based on a ZGR p/n junction. Niu *et al.*[13] reported an even-chain ZGR junction with a parallel magnetization distribution can act as a bipolar spin filter due to the band selective transport. Wang *et al.*[16] proposed an even-chain ZGR junction to produce and detect two 100% polarized spin-up and spin-down currents at two edges of the ribbon. In a recent work,[17] a bipolar spin valve based on a three terminal ZGR junction with different even–odd chain connections was designed to separate and detect one species of spin current. Since the valley valve phenomenon mainly depends on the even–odd chain number of the ZGR, which is difficult to prepare in experiments, one needs to explore a new graphene-like material with a large spin–orbit coupling.

Silicene, a single layer of silicon atoms forming a graphene-like honeycomb lattice, shares almost all the electron transport properties of graphene.[18–26] In particular, the valley valve effect was also predicted in the zigzag silicene nanoribbon (ZSR) p/n junctions[20] and ferromagnetic junctions.[21,22] For instance, Tsai *et al.*[20] proposed a current valve very similar to the graphene one in Ref. [11] to separate spin and valley polarized currents in a ZSR p/n junction, and pointed out the unique band structure under the gate voltage is the main reason for the selective transport of the device. Subsequently, Zhou *et al.*[21] reported a band selective spin filter in a ZSR ferromagnetic junction; they revealed that the valley valve effect mainly comes from the asymmetry edge of the ribbon, and predicted that the spin filter phenomenon exhibits the even–odd chain effect, which are very similar to those in the ZGR junction.

*Project supported by the National Natural Science Foundation of China (Grant No. 11547127), the China Postdoctoral Science Foundation (Grant No. 2017M611852), and the Natural Science Foundation for Colleges and Universities in Jiangsu Province, China (Grant No. 13KJB140005).

†Corresponding author. E-mail: lzhang2010@163.com

© 2018 Chinese Physical Society and IOP Publishing Ltd

Moreover, silicene has a non-planar buckled structure and a large spin–orbit gap of about 1.55 meV,[27] which provides new possibilities for manipulating a massive Dirac fermion around the energy gap electrically.[28] A perpendicular electric field with the Kane–Mele-type spin–orbit interaction can break the structure inversion symmetry of silicene and induce the topological phase transition from the topological insulator to the band insulator,[29] which can be used to filter spin-up and spin-down electrons at different energy valleys.[30–33] For instance, Wang *et al.*[31] reported a theoretical work that a bulk silicene with a spatially alternative electric field can generate a no dissipation spin-dependent valley current. By means of the Keldysh Green function method, Farokhnezhad *et al.*[32] proposed a ZSR ferromagnetic junction with a perpendicular electric field as a perfect spin valve to generate a fully polarized spin current. Recently, the spin switching phenomena caused by electrical tunable edge modes of silicene were also confirmed by the DFT calculations[34–36] and the low-energy electron diffraction experiments.[37]

At present, the spin transport affected by the interplay between the valley valve effect and the controllable band structure of ZSR junction has not received enough attention.[32,33] Thus, in this work, we design a ZSR ferromagnetic junction in Fig. 1 to study the band selective spin transport influenced by a tunable perpendicular electric field in the topological phase transition of silicene. By using the Landauer–Bütticker formula,[38,39] we calculate the spin-resolved conductance spectrum of the system and find that the valley valve effect could exist in an even-chain ZSR junction when the perpendicular electric field is absent and the ZSR is in the topological insulator phase. The ON and OFF states of the spin conductance can be easily changed by the electrical methods. On the other hand, when the perpendicular electric field is nonzero and the ZSR is a band insulator, the spin valve phenomenon remains in the ZSR junction, which does not come from the valley valve effect, but from the energy gap opened by the perpendicular electric field. Furthermore, we also explain the two spin valve phenomena by means of the energy band theory.

The rest of the paper is arranged as follows. In Section 2, we give the detailed theoretical model of the ZSR junction, and derive the general formulae for the spin-dependent conductance of the tunneling junction. In Section 3, we present the numerical results of the spin transport affected by the interplay between the valley valve effect and the tunable energy band of the ZSR junction. We summarize our results in the last section.

2. Model and formulation

We study a ZSR ferromagnetic junction as illustrated in Fig. 1, the whole device consists of three parts: the C nonmagnetic ZSR, the left (L) and right (R) semi-infinite ZSR ferromagnetic electrodes. The left and right ZSR leads have different local magnetization induced by two ferromagnetic insulator substrates. A perpendicular electric field is only applied on the C ZSR region.

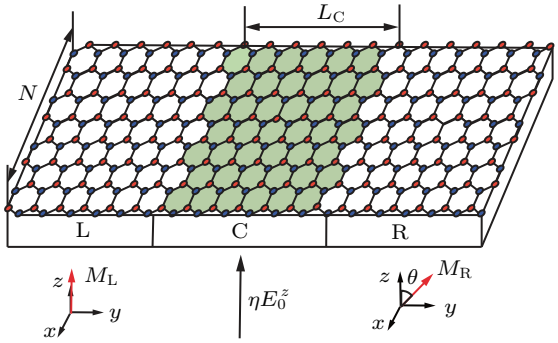


Fig. 1. (color online) Schematic plot of electrical controllable spin valves based on a ZSR ferromagnetic junction. The C region is an undoped ZSR, the left (L) and right (R) electrodes are two semi-infinite ZSRs with different local magnetization $M_{L(R)}$. The perpendicular electric field ηE_0^z is applied on the C ZSR region, which can induce a staggered potential $\eta\Delta_C$ and a weak disordered potential w_i between the A (red dot, $\eta=+1$) and B (blue dot, $\eta=-1$) sublattices of silicene. The width and length of the C ZSR are described by N and L_C, respectively.

The Hamiltonian of the system can be described by the next-nearest-neighbor tight-binding model[18]

$$\begin{aligned} H = & -t\sum_{\langle i,j\rangle\alpha} c_{i\alpha}^{\dagger}c_{j\alpha} - \mathrm{i}\frac{\lambda_{\mathrm{so}}}{3\sqrt{3}}\sum_{\langle\langle i,j\rangle\rangle\alpha\beta} \nu_{ij}c_{i\alpha}^{\dagger}\sigma_{\alpha\beta}^{z}c_{j\beta} \\ & -\mathrm{i}\frac{2}{3}\lambda_R\sum_{\langle\langle i,j\rangle\rangle\alpha\beta}\mu_{ij}c_{i\alpha}^{\dagger}(\boldsymbol{\sigma}\times\hat{\boldsymbol{d}}_{ij})_{\alpha\beta}^{z}c_{j\beta} + \sum_{i\alpha}c_{i\alpha}^{\dagger}(\boldsymbol{\sigma}\cdot\boldsymbol{M})c_{i\alpha} \\ & +\sum_{i\alpha}(\eta_i\Delta_i + w_i)c_{i\alpha}^{\dagger}c_{i\alpha} + \mathrm{c.c.}, \end{aligned} \tag{1}$$

where the 1st term represents the nearest neighbor interaction with the transfer energy t, where $\langle i,j\rangle$ means all the nearest neighbor sites, and $c_{i\alpha(\beta)}^{\dagger}(c_{i\alpha(\beta)})$ creates (annihilates) a quasiparticle with spin index $\alpha(\beta)=\uparrow\downarrow$ at lattice site i. The 2nd term describes the effective spin–orbit coupling with strength λ_{so}, where $\nu_{ij}=\pm1$ for the next-nearest neighbor hopping anti-clockwise (clockwise) around a hexagon with respect to the z axis, and $\boldsymbol{\sigma}=(\sigma^x,\sigma^y,\sigma^z)$ is the Pauli matrix in spin space. The 3rd term denotes the intrinsic Rashba spin–orbit interaction with λ_{R}, $\hat{\boldsymbol{d}}_{ij}$ is a unit vector from the next-nearest neighbor site i to j. The notation $\boldsymbol{\sigma}\cdot\boldsymbol{M}$ in the 4th term depicts the local magnetization of the left and right ZSR leads. The last term means the perpendicular electric field applied on the C ZSR region, which may cause a staggered potential $\eta_i\Delta_{\mathrm{C}}$ and a weak disordered potential w_i between the A ($\eta_i=1$) and B ($\eta_i=-1$) sublattices due to the buckled structure of silicene.

Let us derive the linear conductance in the proposed ZSR device, the spin-dependent current $I_{\mathrm{L}\alpha}$ in the left lead can be obtained by applying the Heisenberg equation of motion[40] and the non-equilibrium Green's function method[41,42]

$$I_{\mathrm{L}\alpha} = \frac{e}{h}\int \mathrm{d}E\mathrm{Tr}[G^{\mathrm{r}}_{\alpha}\Sigma^{<}_{\mathrm{L}\alpha} + G^{<}_{\alpha}\Sigma^{\mathrm{a}}_{\mathrm{L}\alpha} + \mathrm{c.c.}], \tag{2}$$

where e is an electron's charge and $h = 2\pi\hbar$ is the Planck constant. The notation Tr means trace over all the transverse lattices of the C ZSR region. $G^{\mathrm{r,a,<}}_{\alpha}$ and $\Sigma^{\mathrm{r,a,<}}_{\alpha}$ are retarded, advanced, lesser Green's functions, and self-energy matrices, respectively. Using the Hermitian conjugation relations:[38,39] $G^{\mathrm{a}}_{\alpha} = [G^{\mathrm{r}}_{\alpha}]^{\dagger}$, $\Sigma^{\mathrm{a}}_{\alpha} = [\Sigma^{\mathrm{r}}_{\alpha}]^{\dagger}$ and $G^{<}_{\alpha} = -[G^{<}_{\alpha}]^{\dagger}$, equation (2) can be expressed as

$$I_{\mathrm{L}\alpha} = \frac{e}{h}\int \mathrm{d}E\mathrm{Tr}[(G^{\mathrm{r}}_{\alpha} - G^{\mathrm{a}}_{\alpha})\Sigma^{<}_{\mathrm{L}\alpha} + G^{<}_{\alpha}(\Sigma^{\mathrm{a}}_{\mathrm{L}\alpha} - \Sigma^{\mathrm{r}}_{\mathrm{L}\alpha})], \tag{3}$$

By employing the following Keldysh formula:[43,44] $G^{\mathrm{r}}_{\alpha} - G^{\mathrm{a}}_{\alpha} = -\mathrm{i}G^{\mathrm{r}}_{\alpha}(\Gamma^{\mathrm{L}}_{\alpha} + \Gamma^{\mathrm{R}}_{\alpha})G^{\mathrm{a}}_{\alpha}$, $\Sigma^{<}_{\mathrm{L}\alpha} = \mathrm{i}\Gamma^{\mathrm{L}}_{\alpha}f_{\mathrm{L}}$, $\Sigma^{\mathrm{a}}_{\alpha} - \Sigma^{\mathrm{r}}_{\alpha} = -\mathrm{i}\Gamma^{\mathrm{L}}_{\alpha}$ and $G^{<}_{\alpha} = G^{\mathrm{r}}_{\alpha}\Sigma^{<}_{\alpha}G^{\mathrm{a}}_{\alpha}$, equation (3) can be simplified as a two-terminal Landauer–Bütikker formula[38,39]

$$I_{\mathrm{L}\alpha} = \frac{e}{h}\int \mathrm{d}E\mathrm{Tr}[\Gamma^{\mathrm{L}}_{\alpha}G^{\mathrm{r}}_{\alpha}\Gamma^{\mathrm{R}}_{\alpha}G^{\mathrm{a}}_{\alpha}][f_{\mathrm{L}}(E) - f_{\mathrm{R}}(E)], \tag{4}$$

where $\Gamma^{\mathrm{L(R)}}_{\alpha} = \mathrm{i}[\Sigma^{\mathrm{r}}_{\mathrm{L(R)}\alpha} - \Sigma^{\mathrm{a}}_{\mathrm{L(R)}\alpha}]$ is the left (right) linewidth function, which describes the coupling strength between the left (right) lead and the C region. $f_{\mathrm{L(R)}}(E) = 1/(\mathrm{e}^{(E-\mu_{\mathrm{L(R)}})/kT} + 1)$ is the Fermi–Dirac distribution function with the chemical potential $\mu_{\mathrm{L(R)}}$. The linear spin-resolved conductance at zero temperature limit can be defined as

$$\begin{aligned} G_{\mathrm{LR}\alpha} &= \lim_{\mathrm{V}\to 0}\frac{\mathrm{d}I_{\mathrm{L}\alpha}}{\mathrm{d}V} = \frac{e^2}{h}T_{\mathrm{LR}\alpha}(E_{\mathrm{F}}) \\ &= \frac{e^2}{h}[\Gamma^{\mathrm{L}}_{\alpha}(E_{\mathrm{F}})G^{\mathrm{r}}_{\mathrm{LR}\alpha}(E_{\mathrm{F}})\Gamma^{\mathrm{R}}_{\alpha}(E_{\mathrm{F}})G^{\mathrm{a}}_{\mathrm{RL}\alpha}(E_{\mathrm{F}})], \end{aligned} \tag{5}$$

where e^2/h is the unit of the spin-dependent conductance. $T_{\mathrm{LR}\alpha}$ is the transmission coefficient, and $V = \mu_{\mathrm{L}} - \mu_{\mathrm{R}}$ is the external bias between the left and right ZSR electrodes. E_{F} is the Fermi level. $G^{\mathrm{r(a)}}_{\mathrm{LR}\alpha}$ and $G^{\mathrm{r(a)}}_{\mathrm{RL}\alpha}$ are $(N\times N)$-dimensional block matrices of $G^{\mathrm{r(a)}}_{\alpha}$, and the retarded Green's function $G^{\mathrm{r(a)}}_{\alpha}$ can be solved by the matrix inversion directly

$$\begin{aligned} G^{\mathrm{r}}_{\alpha} &= \begin{pmatrix} G^{\mathrm{r}}_{\mathrm{LL}\alpha} & G^{\mathrm{r}}_{\mathrm{LC}\alpha} & G^{\mathrm{r}}_{\mathrm{LR}\alpha} \\ G^{\mathrm{r}}_{\mathrm{CL}\alpha} & G^{\mathrm{r}}_{\mathrm{CC}\alpha} & G^{\mathrm{r}}_{\mathrm{CR}\alpha} \\ G^{\mathrm{r}}_{\mathrm{RL}\alpha} & G^{\mathrm{r}}_{\mathrm{RC}\alpha} & G^{\mathrm{r}}_{\mathrm{RR}\alpha} \end{pmatrix} \\ &= [EI - H_{\mathrm{C}} - \Sigma^{\mathrm{r}}_{\mathrm{L}\alpha} - \Sigma^{\mathrm{r}}_{\mathrm{R}\alpha}]^{-1}, \end{aligned} \tag{6}$$

where H_{C} is the Hamiltonian of the C ZSR region, and I is a unit matrix. The influences of two semi-infinite ZSR leads are merged into the two self-energy terms $\Sigma^{\mathrm{r}}_{\mathrm{L(R)}\alpha}$, which can be calculated by the recursive Green's function method.[45,46] The above calculation of $\Sigma^{\mathrm{r}}_{\mathrm{L(R)}\alpha}$ is only valid when the magnetization direction is along the z axis. If the right ZSR electrode has a magnetization angle θ against the z axis, $\Sigma^{\mathrm{r}}_{\mathrm{R}\alpha}$ should be rotated at angle θ in spin space.

3. Numerical results and discussion

In this section, we mainly focus on the spin-dependent conductance $G_{\mathrm{LR}\alpha}$ and the spin valve phenomena affected by the valley valve effect and the tunable band structure in a ZSR ferromagnetic junction. In the calculations, the zero temperature limit $T = 0$ K is considered. The local magnetizations of the left and right ZSR terminals are set to have the same amplitudes $|M_{\mathrm{L}}| = |M_{\mathrm{R}}| = M = 0.05$ eV, and different orientations $\theta_{\mathrm{L}} = 0$, $\theta_{\mathrm{R}} = \theta$ with respect to the positive z axis. The nearest transfer energy $t = 1.6$ eV, the Rashba spin–orbit coupling coefficient is $\lambda_{\mathrm{R}} = 0.7$ meV and the effective spin–orbit interaction magnitude λ_{so} can be modulated by an external electric field. Because the valley valve effect occurs only in even-chain ZSR junctions and the disordered lattice potential is weak, in most cases unless otherwise stated, the width, the length, and the disordered potential strength of the C ZSR region are fixed $N = 10$, $L_{\mathrm{C}} = 20$, and $w = 0$ eV, respectively.

In Fig. 2, we plot the spin-resolved conductance $G_{\mathrm{LR}\alpha}$ versus Fermi level E_{F} for different system parameters when the perpendicular staggered potential $\Delta_{\mathrm{C}} = 0$ eV. Figures 2(a) and 2(b) describe $G_{\mathrm{LR}\alpha}$ as the function of E_{F} with $\lambda_{\mathrm{so}} = 0$ for the parallel and antiparallel magnetization distributions, respectively. As it is shown, when the zigzag-chain number is even and the magnetization direction is parallel in Fig. 2(a), the spin-up electron is blocked and $G_{\mathrm{LR}\uparrow} = 0$ at the region $E_{\mathrm{F}} \in [0, M]$, the spin-down one meets $G_{\mathrm{LR}\uparrow}(E_{\mathrm{F}}) = G_{\mathrm{LR}\downarrow}(-E_{\mathrm{F}})$ and the prohibited region is $[-M, 0]$. Similar spin valve phenomena emerge in the antiparallel magnetization configuration as shown in Fig. 2(b), $G_{\mathrm{LR}\uparrow} = G_{\mathrm{LR}\downarrow} = 0$ at the region $[-M, M]$, where both spin-up and spin-down electrons are forbidden to flow through the tunneling junction. Similar to that in a ZGR junction,[12,13] the spin valve exhibits the even–odd chain effect, and it could not appear in the odd-chain ZSR junction in Fig. 2(c). In addition, when the disordered lattice potential $w \neq 0$, a conductance peak (valley) appears in the vicinity of $E_{\mathrm{F}} = 0$ for the even (odd)-chain ZSR junction, which means that the weak w cannot break the valley valve effect, but it can affect the ON/OFF states of spin transport around the Fermi zero point. The spin switching effect influenced by an electrical tunable spin–orbit coupling λ_{so} in the antiparallel magnetized ZSR junction is presented in Fig. 2(d), the spin valve phenomenon is still preserved when a weak λ_{so} is applied, the blocked region of the spin transport ($G_{\mathrm{LR}\uparrow} = 0$) is divided into two parts $[-M + \lambda_{\mathrm{so}}, -\lambda_{\mathrm{so}}]$ and $[\lambda_{\mathrm{so}}, M - \lambda_{\mathrm{so}}]$. The width of each forbidden region is reduced to $M - 2\lambda_{\mathrm{so}}$, therefore, it is possible to allow and prohibit the spin transport by electrically modulating the spin–orbit coupling λ_{so}.

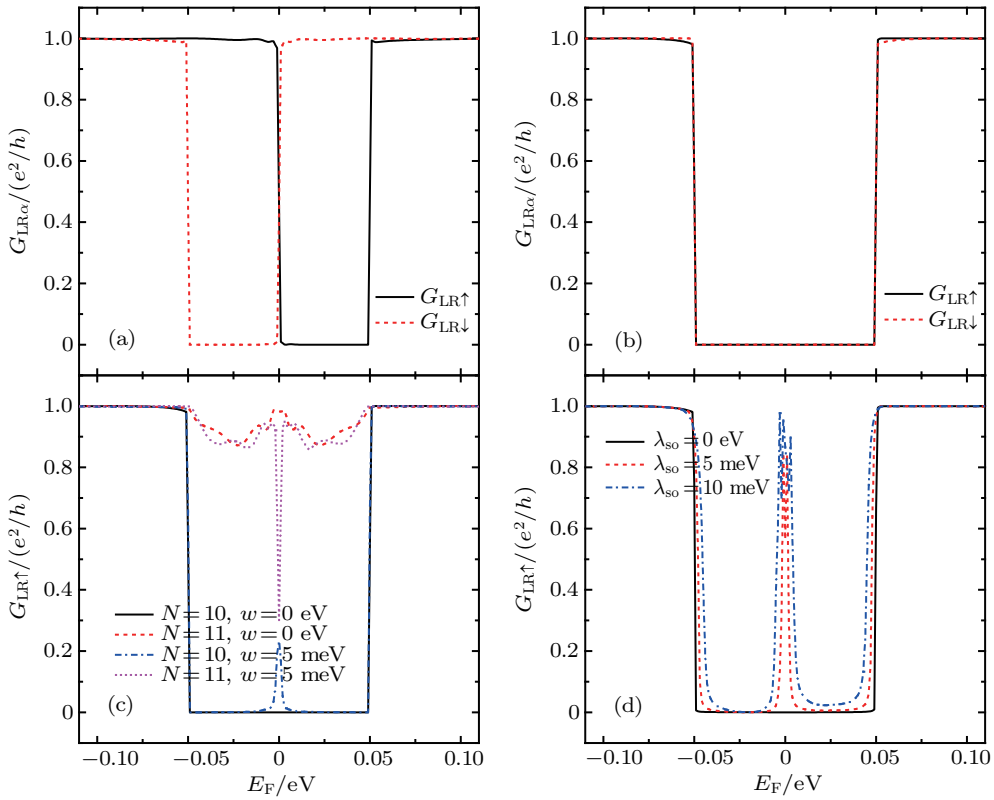


Fig. 2. (color online) Spin-dependent conductance $G_{\mathrm{LR}\alpha}$ versus Fermi level E_{F} in the ZSR ferromagnetic junction for (a) parallel magnetization $\theta = 0$, and (b) antiparallel magnetization $\theta = \pi$. (c) and (d) $G_{\mathrm{LR}\uparrow}$ versus E_{F} for different even–odd chain number N, disordered lattice potential strength w, and effective spin–orbit coupling λ_{so} in the antiparallel magnetized ZSR junction, respectively. The perpendicular staggered potential $\Delta_{\mathrm{C}} = 0$ eV.

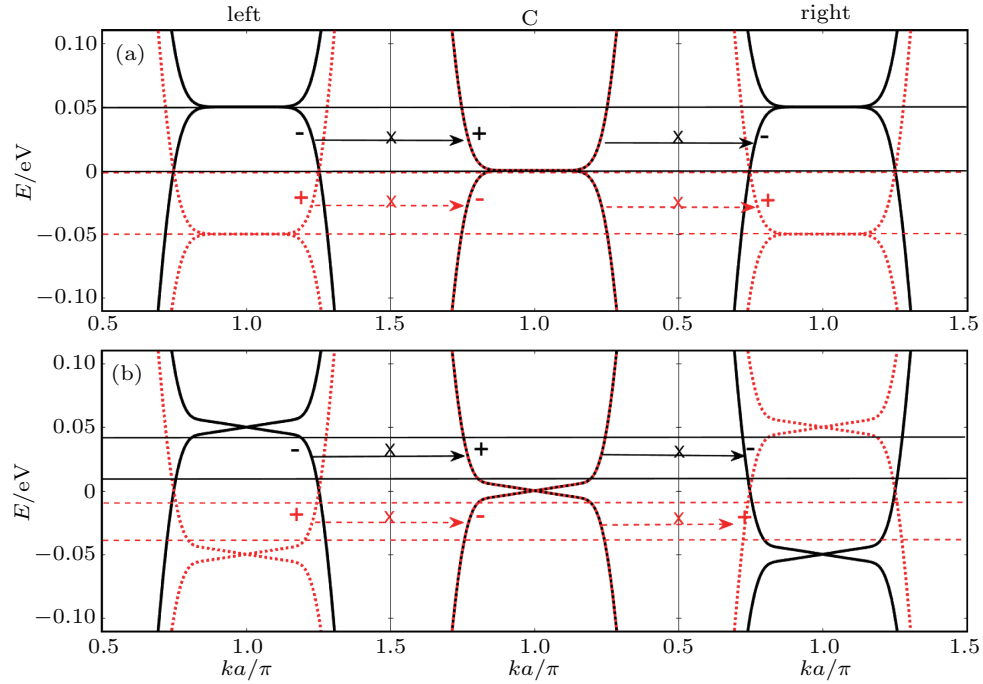


Fig. 3. (color online) Energy–momentum relations of the left (ferromagnetic), C (nonmagnetic), and right (ferromagnetic) ZSRs for (a) $\lambda_{\mathrm{so}} = 0$ eV, $\theta = 0$ and (b) $\lambda_{\mathrm{so}} = 5$ meV, $\theta = \pi$. The "$+(-)$" represents the even (odd) pseudo-parity (symmetry) of the quasi-particle, and it could be different for the conduction bands and the valence bands. The arrows show the electron transport owing to the band selection rule. The areas between two solid (dashed) lines depict the forbidden transport regions of the spin-up (-down) electrons.

We use the energy band theory and pseudo-parity conservation to explain the spin valve phenomena in Fig. 2. The band structures of the left, C, and right ZSRs are plotted in Fig. 3. As it is shown, the ZSRs are gapless semi-metals when the perpendicular electric field Δ_{C} and the spin–orbit coupling λ_{so} are both absent in Fig. 3(a). The spin-up (-down) sub-

bands shift a Zeeman splitting energy $\pm M$ from the Fermi energy zero point, which may cause the spin-up (-down) electrons on the left (right) and C regions to have opposite pseudo-parities within the energy range $[0,M]([-M,0])$ in the parallel magnetized ZSR junction, therefore the valley valve effect appears and the corresponding conductance $G_{\mathrm{LR}\uparrow}(G_{\mathrm{LR}\downarrow}) = 0$ at $[0,M]([-M,0])$, as shown in Fig. 2(a). When the spin–orbit coupling $\lambda_{\mathrm{so}} \neq 0$ and the magnetization orientation is antiparallel in Fig. 3(b), the spin-up and spin-down subbands are exchanged, the energy ranges of the asymmetric pseudo-parities for spin-up and spin-down electrons are both extended to $[-M,M]$. On the other hand, the ZSR is a topological insulator under a weak spin–orbit coupling, its topological edge states (the bands crossing the gap in Fig. 3(b)) $[-\lambda_{\mathrm{so}},+\lambda_{\mathrm{so}}]$ and $[\pm M \mp \lambda_{\mathrm{so}}, \pm M \pm \lambda_{\mathrm{so}}]$ are allowed for the spin transport, due to the interplay between the valley valve effect and the edge state, the spin-up and spin-down conductances are both suppressed at two regions $[-M+\lambda_{\mathrm{so}}, -\lambda_{\mathrm{so}}]$ and $[\lambda_{\mathrm{so}}, M-\lambda_{\mathrm{so}}]$ in Fig. 2(d). For the zigzag-chain number is odd in Fig. 2(c), the valley valve effect of the system disappears, the electron transport no longer satisfies the pseudo-parity conservation, thus the spin-resolved conductances are nonzero in the whole energy region.

We draw the conductance $G_{\mathrm{LR}\alpha}$ as a function of magnetization M for different spin–orbit coupling λ_{so} in the parallel magnetized ZSR junction in Fig. 4(a). As it is shown, there exists a critical magnetization $M_{\mathrm{C}} = E_{\mathrm{F}}$ for filtering one species of spin. When $\lambda_{\mathrm{so}} = 0$ and $M < M_{\mathrm{C}}$, both spin-up and spin-down electrons are permitted to flow through the ZSR junction. When $M > M_{\mathrm{C}}$, only a spin-up electron can transport through the tunneling junction. When $\lambda_{\mathrm{so}} \neq 0$, the topological edge state should be considered, $G_{\mathrm{LR}\downarrow}$ is neither equal to 0 nor equal to 1 in the region $[M_{\mathrm{C}} - \lambda_{\mathrm{so}}, M_{\mathrm{C}} + \lambda_{\mathrm{so}}]$ as also shown in Fig. 4(a). Therefore, the device can be designed as an electrical controllable spin valve by modulating λ_{so}. We also calculate $G_{\mathrm{LR}\alpha}$ versus magnetization angle θ for different λ_{so} around $E_{\mathrm{F}} = M_{\mathrm{C}}$ in Fig. 4(b). When $\lambda_{\mathrm{so}} = 0$, the spin-up electron is allowed to pass through the junction and the spin-down one is completely blocked, i.e., $G_{\mathrm{LR}\uparrow} \neq 0$ and $G_{\mathrm{LR}\downarrow} = 0$. The nonzero conductance $G_{\mathrm{LR}\uparrow}$ is a cosine-like curve of magnetization angle θ, when $\theta = 2k\pi$ with k is an integer, $G_{\mathrm{LR}\uparrow}$ reaches its maximum (minimum) value for the parallel (antiparallel) magnetization configuration. Thus, the parallel magnetized ZSR junction can act as a perfect spin valve to block the spin-down electron when λ_{so} is tuned to 0. When $\lambda_{\mathrm{so}} \neq 0$, the topological edge effect takes effect, both $G_{\mathrm{LR}\uparrow} \neq 0$ and $G_{\mathrm{LR}\downarrow} \neq 0$ no matter how θ changes. Furthermore, two spin conductances are oscillating out of phase with the magnetization angle θ, as also shown in Fig. 4(b).

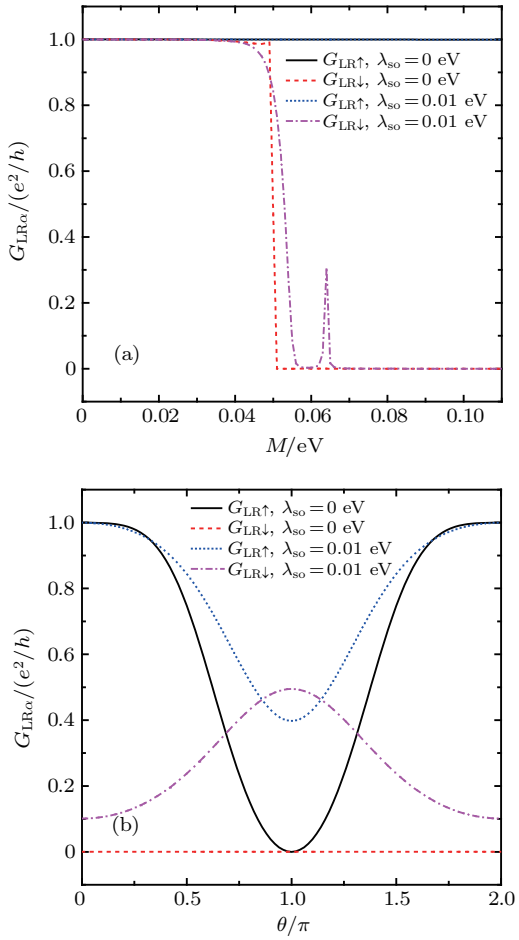


Fig. 4. (color online) (a) $G_{\mathrm{LR}\alpha}$ versus magnetization strength M for different spin–orbit coupling λ_{so}, (b) $G_{\mathrm{LR}\alpha}$ versus magnetization angle θ for different λ_{so} in the parallel magnetized ZSR junction. The other parameters are set as follows: $E_{\mathrm{F}} = 0.05$ eV in panel (a), $E_{\mathrm{F}} = 0.045$ eV in panel (b).

In Fig. 5(a), we give the numerical results of $G_{\mathrm{LR}\alpha}$ versus E_{F} influenced by a nonzero perpendicular staggered potential in the parallel magnetized ZSR junction. When the perpendicular staggered potential $\Delta_{\mathrm{C}} \neq 0$ and spin–orbit coupling $\lambda_{\mathrm{so}} \neq 0$, the spin valve phenomena ($G_{\mathrm{LR}\alpha} = 0$) still appear in the ZSR junction. Different from the case of $\Delta_{\mathrm{C}} = 0$, both spin-up and spin-down conductances are equal to 0 at the same region $[-\Delta_{\mathrm{C}} + \lambda_{\mathrm{so}}, \Delta_{\mathrm{C}} - \lambda_{\mathrm{so}}]$ which cannot be explained by the pseudo-parity conservation of the valley valve effect. To further study the effect of perpendicular staggered potential on the spin transport, we also plot $G_{\mathrm{LR}\alpha}$ of the antiparallel magnetized ZSR junction in Fig. 5(b). The spin-up and spin-down conductances are almost degenerate, and the transport blocked regions are the same as those in the parallel magnetized ZSR junction. Although this current valve can also be tuned by the staggered potential Δ_{C} and the spin–orbit interaction λ_{so}, it can only be used to switch charge current. One cannot further separate and detect spin-up and spin-down currents from the charge current in the above ZSR junction when a nonzero Δ_{C} is applied.

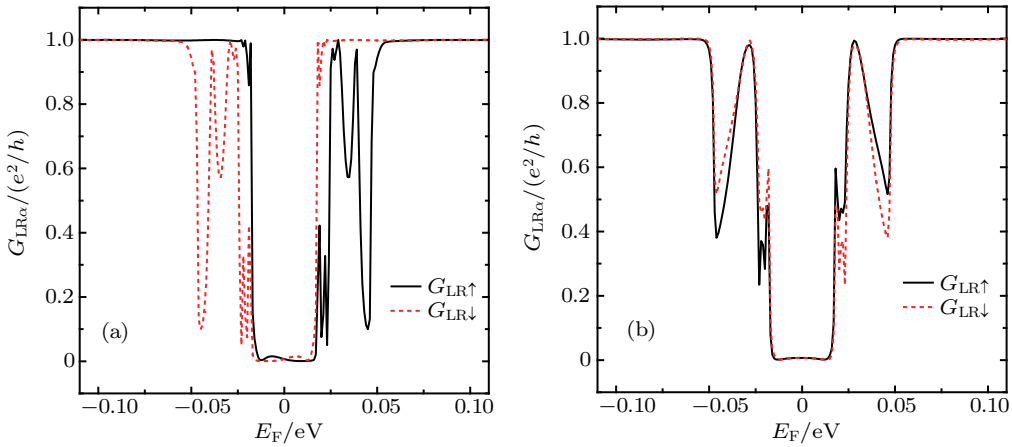


Fig. 5. (color online) (a) $G_{\mathrm{LR}\alpha}$ versus E_{F} for (a) parallel magnetization and (b) antiparallel magnetization under a nonzero perpendicular staggered potential $\Delta_{\mathrm{C}} = 0.02$ eV. The other parameter is $\lambda_{\mathrm{so}} = 5$ meV.

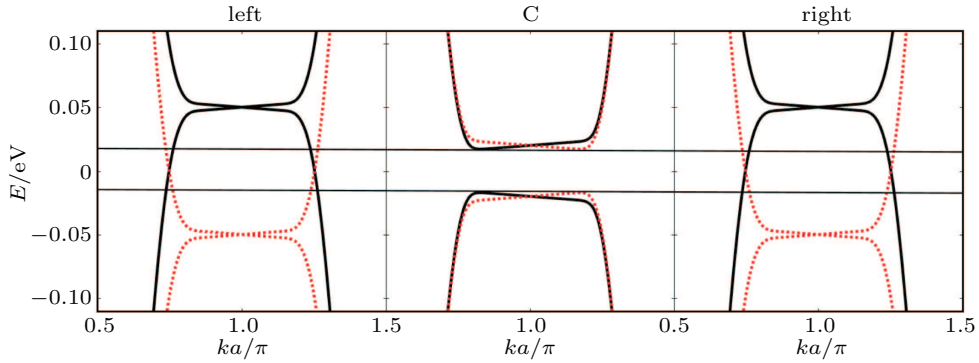


Fig. 6. (color online) Energy band structure of the parallel magnetized ZSR junction under $\Delta_{\mathrm{C}} = 0.01$ eV and $\lambda_{\mathrm{so}} = 5$ meV. The areas between two solid lines $[-\Delta_{\mathrm{C}} + \lambda_{\mathrm{so}}, \Delta_{\mathrm{C}} - \lambda_{\mathrm{so}}]$ are two transport prohibited regions for both spin-up and spin-down electrons. The other parameters and symbols are the same as those in Fig. 3.

To explain the current valve phenomenon under a nonzero staggered sublattice potential in Fig. 5 that is different from the valley valve effect, we draw the energy band of the device in Fig. 6. The C ZSR is a band insulator when a nonzero perpendicular electric field is applied. The staggered sublattice potential induced by perpendicular electric field can open an energy gap with an approximate width $\pm\Delta_{\mathrm{C}}$ around $E_{\mathrm{F}} = 0$ in the C region, the width of the energy gap can be electrically modulated by the spin–orbit coupling λ_{so}. The quasi-particles in the gap cannot produce any current and the conductance is zero. For the parallel magnetized ZSR junction in Fig. 5(a), the gaps of spin-up and spin-down subbands of C ZSR are both opened at $[-\Delta_{\mathrm{C}} + \lambda_{\mathrm{so}}, \Delta_{\mathrm{C}} - \lambda_{\mathrm{so}}]$, therefore $G_{\mathrm{LR}\uparrow} = G_{\mathrm{LR}\downarrow} = 0$ at the same energy regions. Because the width of the energy gap can only be tuned by Δ_{C} and λ_{so}, which is independent of the magnetization distribution, the regions of $G_{\mathrm{LR}\uparrow\downarrow} = 0$ in the antiparallel magnetized junction in Fig. 5(b) are very similar to those in the parallel one.

Finally, we also discuss the spin valve affected by the controllable staggered potential Δ_{C} and the spin–orbit coupling λ_{so} of the antiparallel magnetized ZSR junction in Fig. 7(a). As it is shown, for a given Fermi level E_{F}, when Δ_{C} is weak, that is, $\Delta_{\mathrm{C}} < E_{\mathrm{F}} - \lambda_{\mathrm{so}}$, both spin-up and spin-down electrons can pass through the ferromagnetic junction and $G_{\mathrm{LR}\uparrow\downarrow} \approx 1$, that is because the energy gap opened by Δ_{C} is too small to block the transmission of spin electrons at the Fermi energy. $G_{\mathrm{LR}\uparrow} \approx 1$ and $G_{\mathrm{LR}\downarrow} \approx 0$ in the range $[E_{\mathrm{F}} - \lambda_{\mathrm{so}}, E_{\mathrm{F}} + \lambda_{\mathrm{so}}]$, which can be used to filter the spin-down electron by tuning λ_{so} electrically. When Δ_{C} increases to more than $E_{\mathrm{F}} + \lambda_{\mathrm{so}}$, the gap is big enough and the Fermi level is located within it, therefore, both spin-up and spin-down conductances decrease to 0.

We also plot $G_{\mathrm{LR}\alpha}$ as a function of λ_{so} in the antiparallel magnetized ZSR junction in Fig. 7(b), when $\lambda_{\mathrm{so}} < E_{\mathrm{F}} < \Delta_{\mathrm{C}}$, both spin-up and spin-down electrons are forbidden to transport and $G_{\mathrm{LR}\uparrow\downarrow} \approx 0$, which can be explained that the transmission electron at the Fermi level is within the gap, λ_{so} is so small that it cannot help electrons pass through the tunneling junction. When λ_{so} increases and $E_{\mathrm{F}} < \lambda_{\mathrm{so}} < \Delta_{\mathrm{C}}$, both spin-up and spin-down conductances increase rapidly with the increasing of λ_{so}. When $\lambda_{\mathrm{so}} > \Delta_{\mathrm{C}}$, the spin-dependent conductance decreases with the increasing of λ_{so}, that is because the gap is closed by λ_{so}, no more electrons can participate in the transport. We also draw the spin-polarized degree $\chi \equiv G_{\mathrm{LR}\uparrow} - G_{\mathrm{LR}\downarrow}/G_{\mathrm{LR}\uparrow} + G_{\mathrm{LR}\downarrow}$ versus λ_{so} in the inner of Fig. 7(b), one can manipulate the spin-polarized degree of the electron from about -20% to 50% by using the spin–orbit coupling λ_{so} electrically.

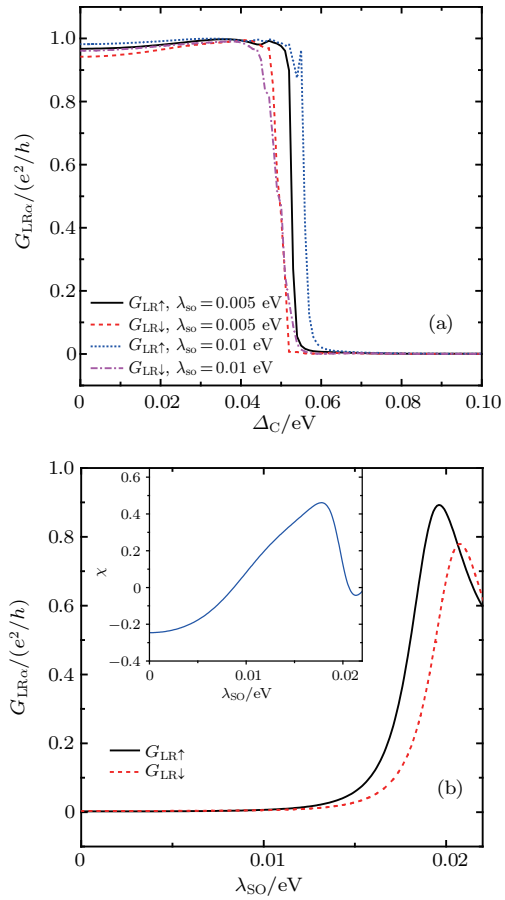


Fig. 7. (color online) (a) $G_{\mathrm{LR}\alpha}$ versus staggered potential Δ_{C} for different spin–orbit interaction strength λ_{so} with $E_{\mathrm{F}} = 0.05$ eV, (b) $G_{\mathrm{LR}\alpha}$ versus λ_{so} with $E_{\mathrm{F}} = 0.01$ eV and $\Delta_{\mathrm{C}} = 0.02$ eV in the antiparallel magnetized ZSR junction. The spin polarization degree χ as a function of λ_{so} is presented in the inner of Fig. 7(b).

4. Summary and conclusion

To conclude, we have investigated the spin valve effect in a ZSR ferromagnetic junction with a perpendicular electric field applied on the C ZSR region. By calculating the spin-resolved conductance of the device, we found that the band selective transport could be preserved in the ZSR junction when the perpendicular electric field is zero and the ZSR is under a topological insulator phase. The valley valve phenomenon in the system emerges as an even–odd chain effect and can be electrically modulated by the Fermi level, the spin–orbit coupling, and the local magnetization. When a nonzero perpendicular electric field is considered, the spin valve phenomenon still exists in the device, but it is mainly determined by the energy gap of the C ZSR, which can be modulated by the interplay between the staggered sublattice potential and the spin–orbit coupling. The proposed device may serve as electrical controllable spin valves or spin filters.

References

[1] Wolf S A, Awschalom D D, Buhrman R A, Daughton J M, von Molnar S, Roukes M L, Chtchelkanova A Y and Treger D M 2001 *Science* **294** 1488

[2] Zutic I, Fabian J and Das Sarma S 2004 *Rev. Mod. Phys.* **76** 323

[3] Awschalom D D and Flatté M E 2007 *Nat. Phys.* **3** 153

[4] Moldovan D, Masir M R, Covaci L, Peeters F M 2012 *Phys. Rev. B* **86** 115431

[5] Novoselov K S, Geim A K, Morozov S V, Jiang D, Katsnelson M I, Grigorieva I V, Dubonos S V and Firsov A A 2005 *Nature* **438** 197

[6] Yang T Y, Balakrishnan J, Volmer F, Avsar A, Jaiswal M, Samm J, Ali S R, Pachoud A, Zeng M, Popinciuc M, Guntherodt G, Beschotem B and Ozyilmaz B 2011 *Phys. Rev. Lett.* **107** 047206

[7] Hwang E H, Adam S and Das Sarma S 2007 *Phys. Rev. Lett.* **98** 186806

[8] Xia F N, Farmer D B, Lin Y M and Avouris P 2010 *Nano Lett.* **10** 715

[9] Raes B, Scheerder J E, Costache M V, Bonell F, Sierra J F, Cuppens J, Van de Vondel J and Valenzuela S O 2016 *Nat. Commun.* **7** 11444

[10] Katsnelson M I, Novoselov K S and Geim A K 2006 *Nat. Phys.* **2** 620

[11] Rycerz A, Tworzydlo J and Beenakker C W J 2007 *Nat. Phys.* **3** 172

[12] Akhmerov A R, Bardarson J H, Rycerz A and Beenakker C W J 2008 *Phys. Rev. B* **77** 205416

[13] Niu Z P and Xing D Y 2010 *Eur. Phys. J. B* **73** 139

[14] Chen J, Cheng S, Shen S Q and Sun Q 2010 *J. Phys.: Condens. Matter* **22** 035301

[15] Wang J, Tian H Y, Yang Y H and Chan K S 2012 *Phys. Rev. B* **86** 081404

[16] Wang Z F, Jin S and Liu F 2013 *Phys. Rev. Lett.* **111** 096803

[17] Zhang L 2017 *J. Phys.: Condens. Matter* **29** 055304

[18] Liu C C, Feng W X and Yao Y G 2011 *Phys. Rev. Lett.* **107** 076802

[19] Vogt P, De Padova P, Quaresima C, Avila J, Frantzeskakis E, Asensio M C, Resta A, Ealet B and Le Lay G 2012 *Phys. Rev. Lett.* **108** 155501

[20] Tsai W F, Huang C Y, Chang T R, Lin H, Jeng H T and Bansil A 2013 *Nat. Commun.* **4** 1500

[21] Zhou B, Zhou B, Chen X W, Liao W and Zhou G 2015 *J. Phys.: Condens. Matter* **27** 465301

[22] Zhai X and Jin G J 2016 *J. Phys.: Condens. Matter* **28** 355002

[23] Shen M, Zhang Y Y, An X T, Liu J J and Li S S 2014 *J. Appl. Phys.* **115** 233702

[24] Deng X Q, Zhang Z H, Tang G P, Fan Z Q and Yang C H 2014 *Rsc Adv.* **4** 58941

[25] Wang Y Y, Quhe R G, Yu D P and Lü J 2015 *Chin. Phys. B* **24** 087201

[26] Wirth-Lima A J, Silva M G and Sombra A S B 2018 *Chin. Phys. B* **27** 023201

[27] Drummond N D, Zolyomi V and Fal'ko V I 2012 *Phys. Rev. B* **85** 075423

[28] Tao L, Cinquanta E, Chiappe D, Grazianetti C, Fanciulli M, Dubey M, Molle A and Akinwande D 2015 *Nat. Nanotechnol.* **10** 227

[29] Ezawa M 2012 *New J. Phys.* **14** 033003

[30] An X T, Zhang Y Y, Liu J J and Li S S 2013 *Appl. Phys. Lett.* **102** 213115

[31] Wang S K, Wang J and Chan K S 2014 *New J. Phys.* **16** 045015

[32] Farokhnezhad M, Esmaeilzadeh M, Ahmadi S and Pourmaghavi N 2015 *J. Appl. Phys.* **117** 173913

[33] Rashidian Z, Hajati H, Rezaeipour S and Baher S 2017 *Physica E* **86** 111

[34] Chowdhury S and Jana D 2016 *Rep. Prog. Phys.* **79** 126501

[35] Majumdar A, Chowdhury S, Nath P and Jana D 2014 *Rsc Adv.* **4** 32221

[36] Das R, Chowdhury S, Majumdar A and Jana D 2015 *Rsc Adv.* **5** 41

[37] Chuang F C, Hsu C H, Chou H L, Crisostomo C P, Huang Z Q, Wu S Y, Kuo C C, Yeh W C V, Lin H and Bansil A 2016 *Phys. Rev. B* **93** 035429

[38] Entin-Wohlman O, Aharony A and Levinson Y 2002 *Phys. Rev. B* **65** 195411

[39] Datta S 1995 *Electronic Transport in Mesoscopic systems*, 2nd edn. (England: Cambridge University Press) pp. 102–103

[40] Lee M H 2000 *Phys. Rev. Lett.* **85** 2422

[41] Datta S 2000 *Superlattices Microstruct.* **28** 253

[42] Pecchia A, Penazzi G, Salvucci L and Di Carlo A 2008 *New J. Phys.* **10** 065022

[43] Haug H and Jauho A P 1999 *Quantum Kinetics in Transport and Optics of Semiconductors* (Berlin: Springer) pp. 162–163

[44] Jauho A P, Wingreen N S and Meir Y 1994 *Phys. Rev. B* **50** 5528

[45] Thorgilsson G, Viktorsson G and Erlingsson S I 2014 *J. Comput. Phys.* **261** 256

[46] Rotter S, Tang J Z, Wirtz L, Trost J and Burgdorfer J 2000 *Phys. Rev. B* **62** 1950